EUROFUSION WPMAT-PR(15) 13824

T. Palacios et al.

Tungsten-vanadium-yttria alloys for fusion power reactors (II): mechanical characterization

Preprint of Paper to be submitted for publication in
International Journal of Refractory Metals and Hard Materials

This work has been carried out within the framework of the EUROfusion Consortium and has received funding from the Euratom research and training programme 2014-2018 under grant agreement No 633053. The views and opinions expressed herein do not necessarily reflect those of the European Commission.

Tungsten-vanadium-yttria alloys for fusion power reactors (II): mechanical characterization

T. Palacios, J.Y. Pastor
Materials Science Department-CIME
Universidad Politécnica de Madrid
E.T.S. de Ingenieros de Caminos, Canales y Puertos
C/Profesor Aranguren, s.n. E28040-Spain

Abstract

In this second part of the study, the aim is to evaluate the influence of adding 2 or 4 wt.% vanadium (V) and 0.5 wt.% yttria (Y_2O_3) to pure tungsten (W) and its effect on their mechanical properties at high temperature, which microstructure at room temperature we have analysed in the first part. These W-based alloys were processed by powder metallurgy and consolidated by hot isostatic pressing (HIP). Smooth and single edge laser-notched beam (SELNB) specimens were tested to determine mechanical strength, yield strength and fracture toughness. To that end, we have performed three-point bending (TPB) tests in both oxidising and vacuum atmosphere in a temperature range from 77 K, obtained via immersion in liquid nitrogen, to 1473 K. Additionally, hardness and elastic modulus were measured via Vickers microindentation and impulse excitation technique (IET), respectively. These results were compared with nanoindentation tests to determine the possible size effect in both parameters. To conclude, fracture surfaces of the tested alloys at different temperatures were analysed with a field emission scanning electron microscopy (FE-SEM). The microscope was useful to establish the link between the macroscopic behaviour and the micromechanisms of failure.

Results show an increase of the mechanical properties in all the temperature range lead by the addition of V and Y_2O_3 to W. The formation of a W-V solid solution benefits the conglomeration of the material and drastically reduces porosity, whereas Y_2O_3 helps to stabilize high temperature degradation. The combination of both alloying elements creates a synergistic effect that triple the microhardness and flexural strength values in comparison with pure W produced by the same powder metallurgy route.

1. Introduction

During last decades, fusion power reactors have drawn enormous attention as a future source of clean energy. As compared to fission reactors, this energy will be capable to meet our future needs with a negligible irradiation effect on our living environment. However, the operation of this technology will impose very demanding conditions, especially for those materials in contact with plasma (PFMs). Particle and heat loads from fusion plasma and neutron loads during reactor operation will enforce extreme conditions and partially contradictory requirements that few materials can satisfy [1]. In addition, these materials for high temperature applications suffer from restricted thermal operation window defined by the ductile-brittle transition temperature (DBTT) and the recrystallization temperature (RT) that should be taken into consideration.

Due to its high melting point, good thermal conductivity, high temperature strength, low thermal expansion and low activation under neutron irradiation W materials and alloys are considered as candidate materials for these plasma-facing components (PFCs) [2]. However, the inherent brittleness of W is a critical drawback for structural applications. Its DBTT is ranged from 473 to 673 K, depending on the fabrication route or determination method; hence the alloying with other elements such as Ta, V, Ti, Re or oxide dispersion-strengthened (ODS) particles like Y_2O_3 or La_2O_3 became necessary to improve its behaviour. In particular, the addition of V in W improves mechanical properties and reduces irradiation damages; however, this theory is only verified by simulations but not experimentally [3]. Furthermore, the addition of Y_2O_3 improves the mechanical properties at high temperature because it minimizes the thermal degradation [4].

2. Materials and samples

We have studied two W based alloys and a pure W material, used as reference. Alloys had a target composition of W-2 wt.% V-0.5 wt.% Y_2O_3 and W-4 wt.% V-0.5 wt.% Y_2O_3, hereafter referred to as W2V0.5Y and W4V0.5Y. All materials were prepared following a powder metallurgy route of mechanical alloying (MA) and subsequent hot isostatic pressing (HIP) procedure describe elsewhere [5]. From this fabrication process, cylinders with dimensions of 30 mm diameter and 50 mm in length were obtained. These cylinders were cut by refrigerated electro-discharge machining (EDM) to obtain bend bar specimens with nominal dimensions of 1.6 x 1.6 x 25 mm^3. Such specimens were used to perform all measurements and experimental methods.

3. Experimental methods

Following ASTM Standard 384-89, we have performed Vickers tests to measure microhardness of the compacted materials. Two loads, 0.98 and 9.8 N, with an application time of 12 s were used to determine the influence of the applied force on the results. After removing the indenter from the surface, lengths of the indentation diagonals were measured via optical microscopy.

Nanoindentation tests were also performed by using a NanoIndenter XP from former MTS Systems Corporation (Oak Ridge, TN, USA) equipped with a Berkovich tip. The Oliver and Pharr method [6] was used to calculate form force-displacement curves nanohardness (H_n) and elastic modulus (E_n) of materials at room temperature. These results were comparable to those obtained via Vickers tests for the hardness and IET method for the elastic modulus (E_{IET}), which uses the natural vibration frequencies of the material [7]. Additionally, we have used a model of maximum values [8] under the hypothesis of isodeformation to get an approximation of the theoretical elastic modulus (E_{th}) as follows:

$$E_{th} = E_W V_W + E_V V_V + E_{Y2O3} V_{Y2O3} + E_{air} V_{air} \quad (2)$$

where E_x represent the elastic modulus (E_W = 400 GPa [9], E_v = 128 GPa [9], E_{Y2O3} = 177 GPa **Error! Reference source not found.** and E_{air} = 0 GPa, respectively, and V_x the volumetric fraction of the corresponding elements in the alloy.

Non-standard three-point bending (TPB) tests were performed on smooth and laser-notched bend bars in a universal testing machine. Tests in air (oxidising atmosphere) were performed in a temperature range between 77 K, obtained via liquid nitrogen immersion, and 1273 K; tests performed under vacuum (inert atmosphere) were undertaken between 673 and 1473 K with a pressure of approximately 10^{-6} mbar.

The bending fixture of the testing machine, connected to the frame using Al_2O_3 load bars, was placed in a high-temperature furnace during the mechanical tests. These TPB tests were realized using load spans for smooth and laser-notched bars of 16.0 and 8.5 mm [12], respectively. They were performed using displacement control with a cross-head speed of 100 µm/min and a heating rate of 30 K/min. Once the set point temperature was reached, a dwell time of 10 min was used to thermally stabilise the system. We continuously monitored load and load point displacement during tests using a load cell and linear variable differential transformer induction transducer, respectively. Three to five samples were tested per material and temperature to ensure repeatability.

Force-displacement data obtained from TPB tests were computed with the standard Euler-Bernoulli equations for slender beams up to failure [11] to obtain σ-ε curves, which determine the maximum tensile bending strength at the fracture point. Because this method is restricted to the elastic bending regime, we used the 0.2 % yield strength offset criteria in the cases where ductile behaviour was exhibited, which especially occurs at higher temperatures.

Single edge laser-notched beam (SELNB) specimens were used to measure fracture toughness by TPB tests on the materials. This method uses a femptosecond laser to produce crack-like notches on fracture toughness samples, it is considered the most suitable to achieve real fracture toughness values in nanostructured materials [12]. As a result, this technique produced notch root radius between 5-20 nm and length notches around 250 µm, although the specific initial notch length was measured via field emission scanning electron microscopy (FE-SEM) for each specimen. Using these values

and the measured maximum load for each test, fracture toughness values (K_{IC}) were calculated by applying the stress intensity factor formula [13].

Finally, to establish the relationship between the mechanical properties obtained with the micromechanisms of failure, a detailed analysis of the fracture surfaces after TPB tests was performed.

4. Results and discussion

4.1 Mechanical properties

A synergistic effect on resulting microhardness was observed with the addition of V and Y_2O_3. W2V0.5Y and W4V0.5Y alloys exhibited values surprisingly higher than those obtained for pure W (Fig. 1). These results, around 12 GPa, were much higher than for previously reported W-based alloys with only one of the alloying elements: W1Y [14], W2V [4] and W4V [unpublished][15]. No significant differences between methods were observed; results from Vickers tests were within the margin of error whereas results from nanoindentation tests were slightly higher. In the comparison of these results with literature data, it is observed 30-40 % lower values for Vickers microhardness in W materials with V addition produced by SPS reported by Arshad [16].

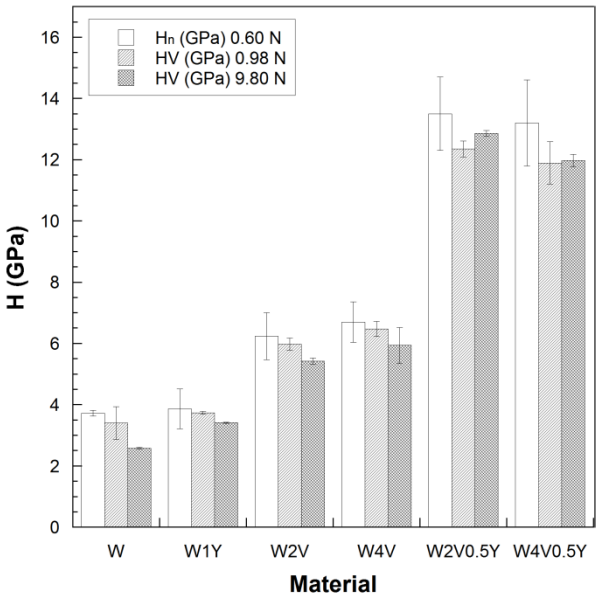

Fig. 1 Vickers microhardness (HV) for two different applied loads and the Berkovich nanohardness (H_n) for W2V0.5Y and W4V0.5Y alloys and the comparison with the reference pure W, previous results of W1Y [4], W4V [14] and W2V (unpublished data).

The resultant elastic modulus from nanoindentation tests (E_n) in comparison with pure W was nearly the same for W4V0.5Y and slightly higher for W2V0.5Y. Similar behaviour was obtained in the case of IET tests (E_{IET}), almost the same values for W4V0.5Y and slightly higher for W2V0.5Y (Fig. 2). In general, the discrepancy between W2V0.5Y and W4V0.5Y alloys was slightly more pronounced than for previous W2V and W4V alloys also because of the increasing porosity of W4V0.5Y [17]. Above all, differences between techniques were very small and the agreement between methods was considered good.

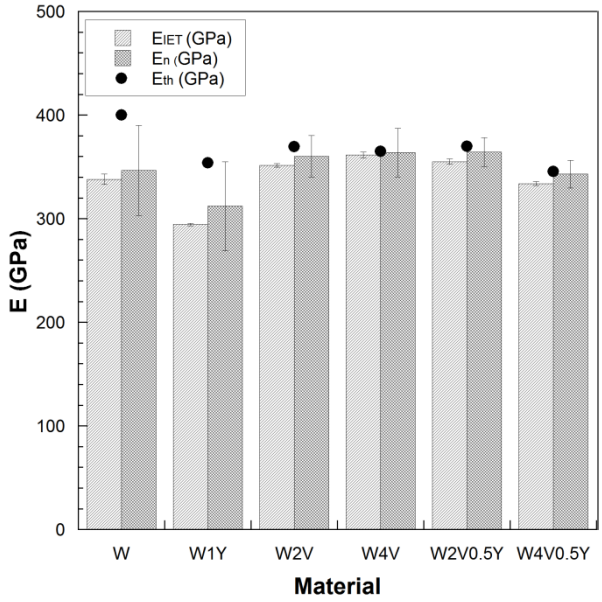

Fig. 2 Elastic modulus measured via IET (E_{IET}), instrumented indentation (E_n) and theoretical calculated (E_{th}) for the W2V0.5Y and W4V0.5Y alloys and the comparison with the reference pure W, previous results of W1Y [4], W4V [14] and W2V (unpublished data).

TPB test results for flexural strength showed values around three times higher than for pure W in all the temperature range, in air and under vacuum (Fig. 3). Both alloys exhibited similar tendency, with some exceptions, in almost all the temperature range. In air (Fig. 3, left), W2V0.5Y alloy exhibited values quite similar than the W4V0.5Y up to 1073 K, temperature at which the alloy reached a maximum flexural strength of 1 GPa; at this same temperature, values obtained for the W4V0.5Y alloy are 30% lower (around 700 MPa). Under vacuum (Fig. 3, right) meanwhile, W2V0.5Y alloy yielded reduced flexural strength relative to those in air, this fact is attributed to blunting of surface defects as explained in [4]. Only at test higher temperatures (i.e. 1473 K), where oxidation in air along the samples was massive, values under vacuum reached higher values than those obtained in air. However for W4V0.5Y, high vacuum results were over those in air in all the temperature range with the only exception of test performed at 1073 K.

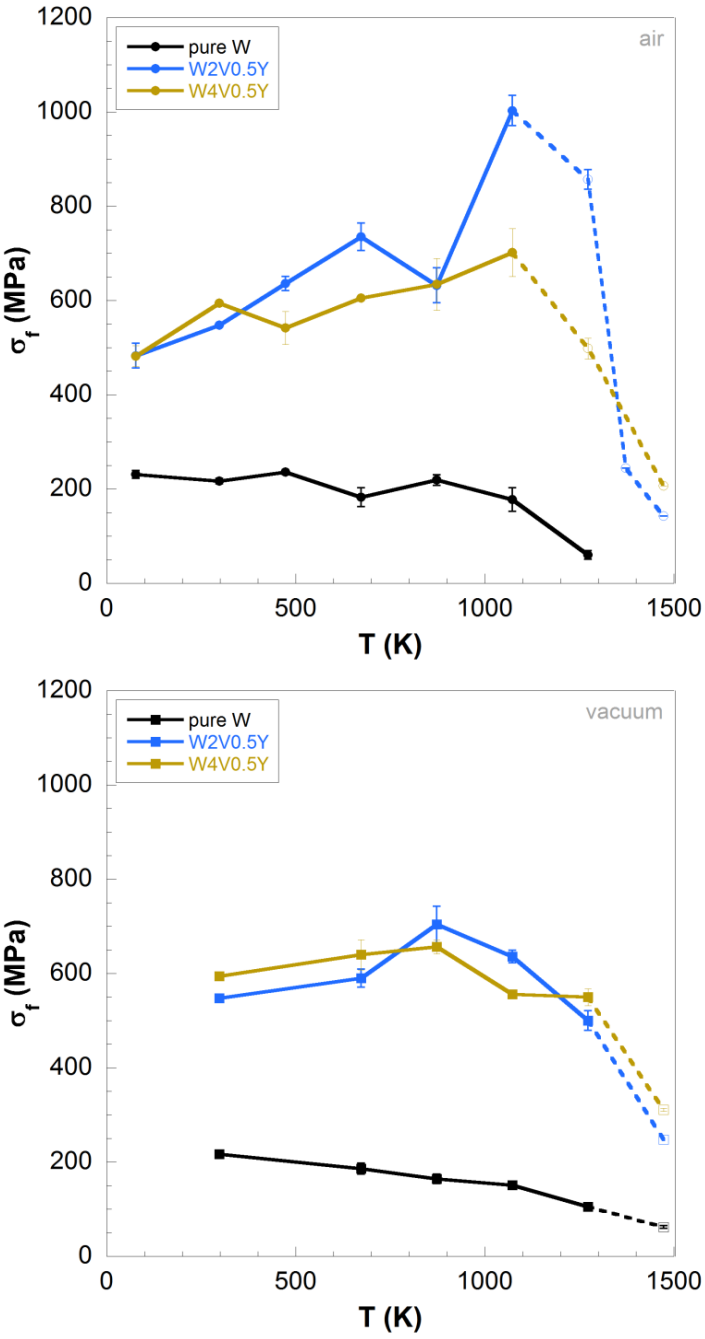

Fig. 3 Average flexural strength as a function of temperature for W2V0.5Y and W4V0.5Y alloys and pure W in air (upper) and under vacuum (bottom). The open symbols and dashed lines represent the yield strength at 0.2 % when the materials exhibited ductile behaviour (Fig. 4).

DBTT can be defined as when σ-ε curves from TPB tests (Fig. 4) changed their behaviour from linearly elastic to plastic, for a given strain rate. In oxidising atmosphere, we have observed a linearly elastic behaviour until failure up to the maximum flexural strength values for both alloys, and only plastic deformation above 1073 K. Under vacuum, however, the plastic behaviour appeared above 1273 K, not only for the alloys but also for pure W. Consequently, DBTT for the studied V-Y_2O_3 alloys lied above 1073 K in air and 1273 K under vacuum. In the cases where σ-ε curves presented plastic behaviour, the 0.2 % yield strength offset was represented using open symbols and dashed lines (Fig. 3). In comparison with pure W, DBTT under vacuum was the same but a slight improvement was observed in air where linear elastic behaviour was observed even at test performed at 1273 K.

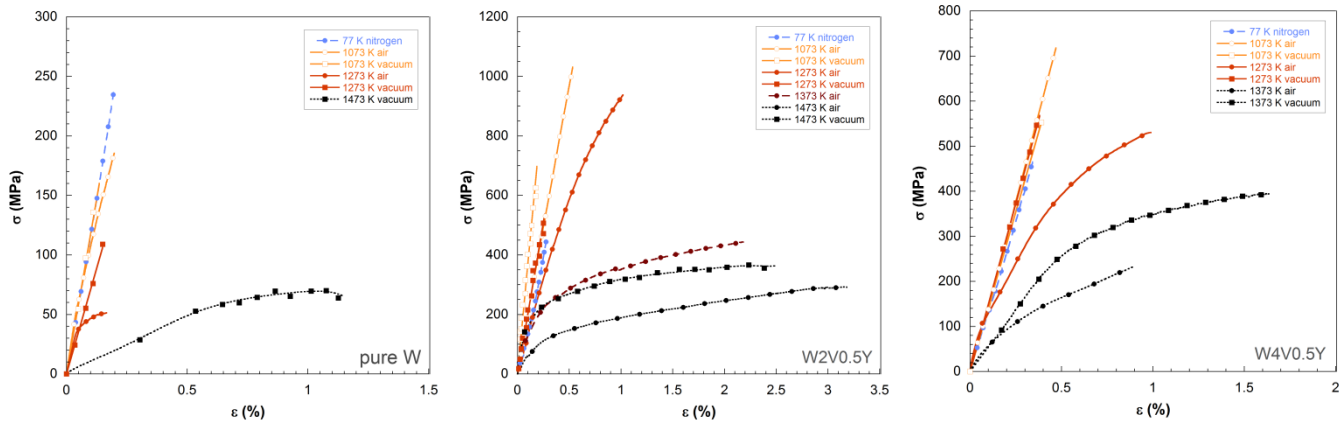

Fig. 4 Representative flexural σ-ε curves at different temperatures of pure W (left), W2V0.5Y (middle) and W4V0.5Y (right). The unrepresented curves had similar linear elastic behaviour up to those one shown in the figure. Note that the scale of the plots is not the same for each material but it is adjusted to the results.

Force-displacement curves obtained from the TPB tests using the SELNB samples exhibited lineal elastic behaviour until fracture for all the temperature range in a similar tendency than curves for flexural strength tests. Average fracture toughness results (Fig. 5) showed an improvement for both alloys that reached values two times higher than those exhibited for pure W. Although results obtained for W4V0.5Y were slightly lower than for W2V0.5Y, the standard error is overlapped in most of the cases. The maximum value of 9.5 MPa·$m^{1/2}$ is given in the W4V0.5Y alloy tested at 873 K in air. It can be observed that oxidation is relevant over 673 and 873 K for W2V0.5Y and W4V0.5Y, respectively, since vacuum surpassed air values over those temperatures.

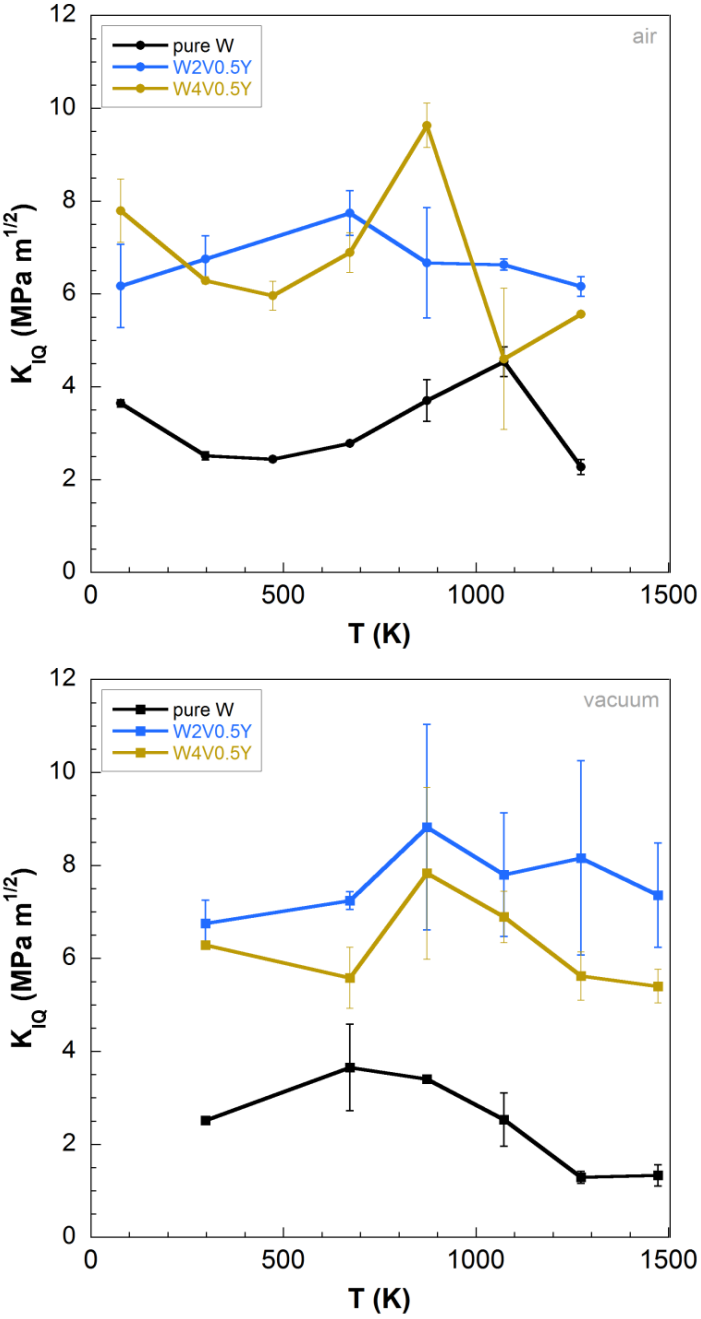

Fig. 5 Average fracture toughness as a function of temperature for W2V0.5Y and W4V0.5Y alloys and pure W in air (upper) and under vacuum (bottom).

4.2 Fracture surfaces

According to ε-σ curves from TPB tests (Fig. 4), fracture surfaces at 300 K (Fig. 6) showed brittle fracture. This is also in agreement with the observed in the macroscopic level, surfaces of all the studied materials exhibited flat breakage in a perpendicular plane to the maximum traction stress without plastic deformation. In the microscopic level meanwhile, surfaces from pure W showed coarse grains with intergranular breakage; decohesion between grain boundaries is supported with the high porosity between grains (reported in [17]) that weaken the union and the inherent fragility of W. Surfaces from W-V-Y alloys at 300 K (Fig. 6), middle and right), showed a rough nanostructured area surrounding some coarse W particles. In certain cases these coarse grains were aligned forming elongated shapes also seen in the micrographs. The fracture mechanism of failure was mainly intergranular, but some cleavage was observed in the coarse W grains (see arrows in Fig. 6, right).

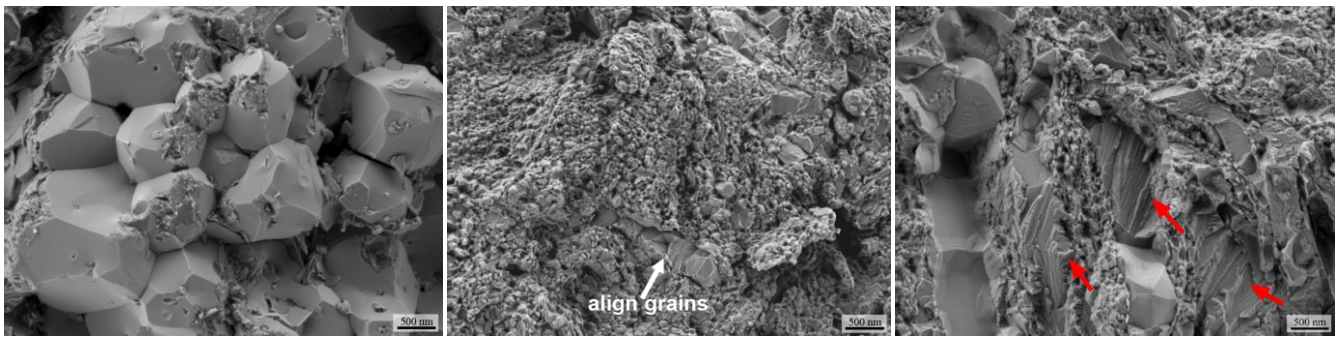

Fig. 6 Fracture surface of pure W (left), W2V0.5Y (middle) and W4V0.5Y (right) at 300 K. Arrows in the micrograph of the W4V0.5Y alloy show transgranular fracture of coarse W grains.

Tests performed in air maintained fracture micromechanisms at least until 673 K. From this temperature, thermal degradation started and a layer of oxides masked fracture surfaces. At 873 K the oxide scale is large enough to cover the whole surfaces (Fig. 7), although oxidation became more evident with increasing temperature and at 1273 K the surface is completely covered (Fig. 8). Due to this, failure micromechanisms cannot be distinguished, but some changes between surfaces can be observed. In pure W surface, non-protective columnar oxides grew from the surface to the outside [18][19], whereas W-V-Y alloys exhibited round particles covering the surface; phenomenon that was more evident with the increasing temperature (Fig. 7, 8). However, no differences were observed between surfaces of W2V0.5Y and W4V0.5Y alloys. A beneficial effect of the addition of Y_2O_3 to W regarding thermal stability was previously reported [4], but no evidences of such protection were found on the alloys, perhaps as a consequence of the joint addition of Y_2O_3 and V.

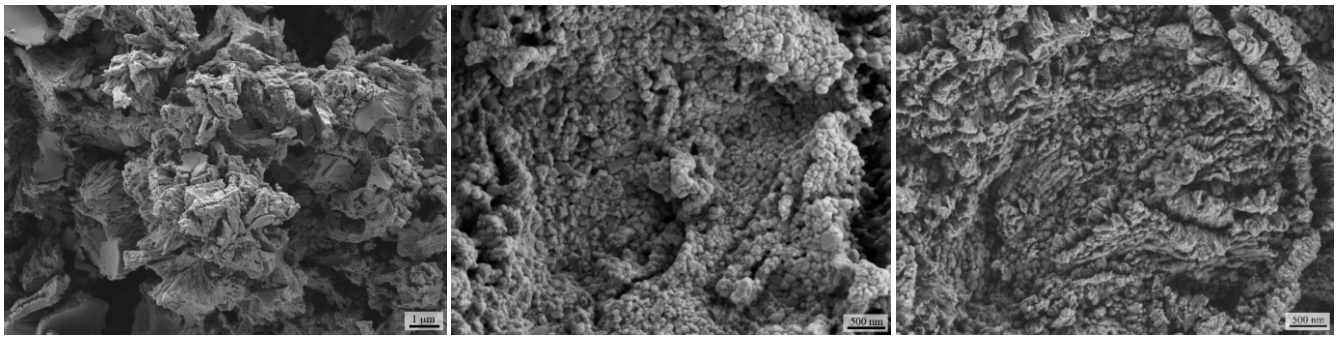

Fig. 7 Fracture surface of pure W (left), W2V0.5Y (middle) and W4V0.5Y (right) at 873 K in oxidising atmosphere (air). Note that because of the difference between grain size of pure W and the alloys, pure W image is shown with less magnification.

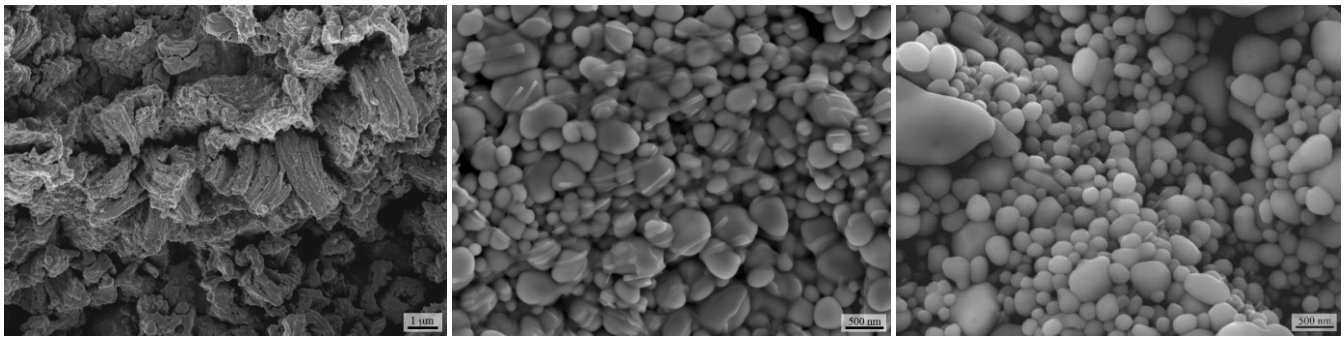

Fig. 8 Fracture surface of pure W (left), W2V0.5Y (middle) and W4V0.5Y (right) at 1273 K in oxidising atmosphere (air). Note that because of the difference between grain size of pure W and the alloys, pure W image is shown with less magnification.

Fracture surfaces of tests performed under vacuum exhibited similar micromechanisms of failure than tests performed at room temperature. In the macroscopic scale, surfaces were mainly flat without evidences of plastic deformation, although specimens of both alloys tested at 1473 K were slightly deformed around the section where force was applied, results that are in concordance with ε-σ curves (Fig. 3, right). In the microscopic scale, the high percentage of cleave grains observed at 300 K in the alloys decreased with the increasing test temperature. At 473 K (Fig. 9) and 673 K (Fig. 10), below the DBTT, cleavage was observed, but it should be noted that was found at 1473 K (Fig. 11), temperature at which alloys were above the DBTT and plastic behaviour was observed in the TPB test results. Beyond this, the main fracture micromechanism was

brittle fracture by grain boundary decohesion. At this high temperature, 1473 K, pure W surfaces experienced grain growth with grains twice the size of those at 300 K. Fracture surfaces of W-V-Y alloys are similar, dark areas of V pools and coarse W grains surrounded by a nanostructured area. Variances were due to the increment (to 4 %) of the V that made V pools more evident.

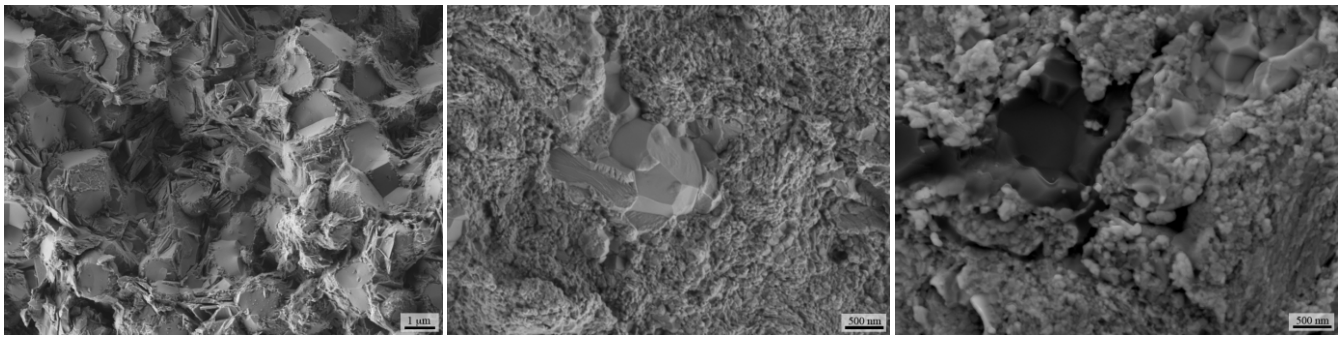

Fig. 9 Fracture surface of pure W (left), W2V0.5Y (middle) and W4V0.5Y (right) at 673 K in vacuum atmosphere (inert). Note than for a better understanding of the surfaces, pure W image is shown with less magnification.

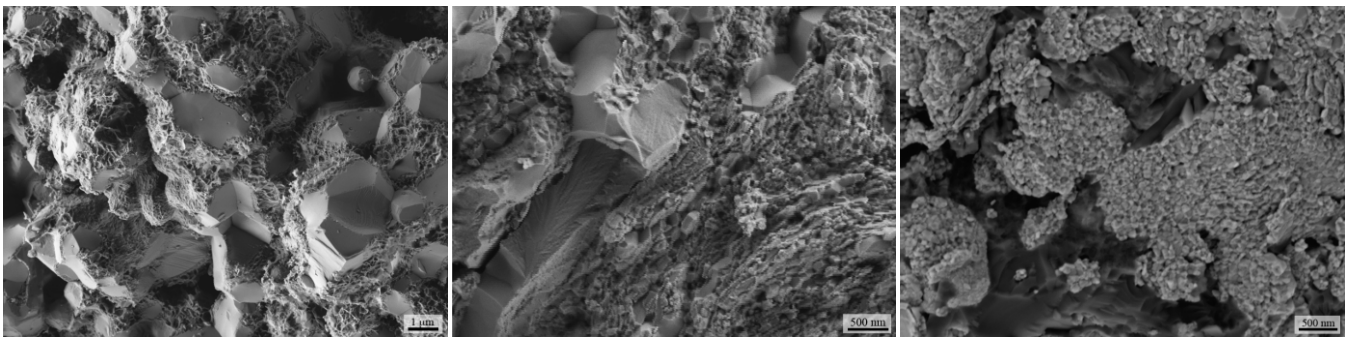

Fig. 10 Fracture surface of pure W (left), W2V0.5Y (middle) and W4V0.5Y (right) at 873 K in vacuum atmosphere (inert). Note than for a better understanding of the surfaces, pure W image is shown with less magnification.

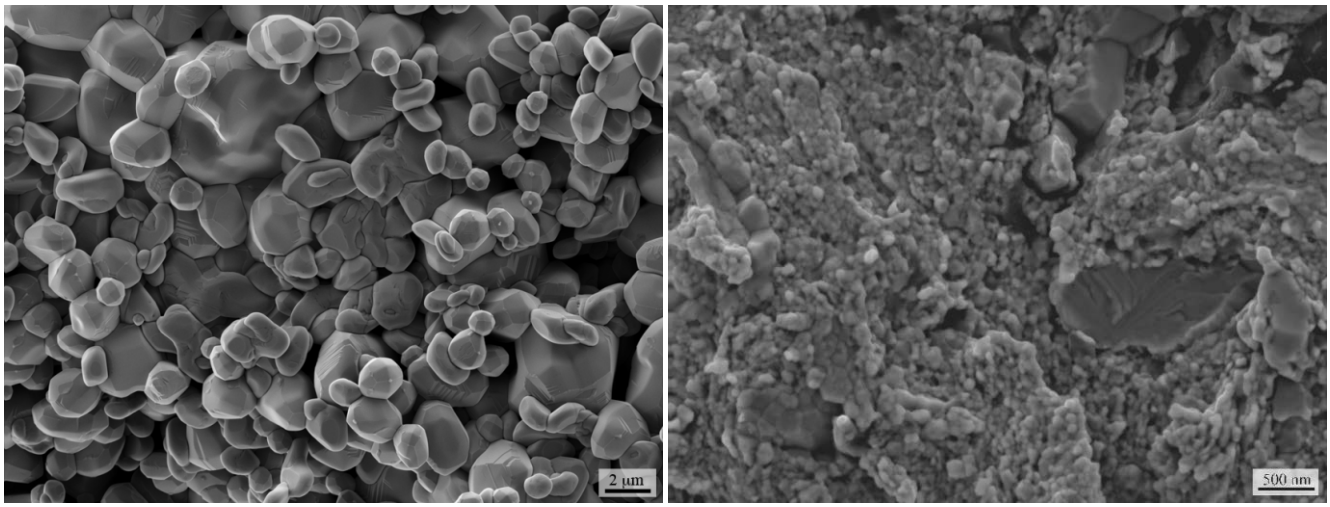

Fig. 11 Fracture surface of pure W (left) and W2V0.5Y (right) at 1473 K in vacuum atmosphere (inert). Note that because of the difference between grain size of pure W and the alloys, pure W image is shown with less magnification. Fracture surface of W4V0.5Y is similar than W2V0.5Y.

5. Conclusions

This study demonstrated the effect of adding 2 or 4 wt.% V and 0.5 wt.% Y_2O_3 to pure W produced by mechanical alloying (MA) and hot isostatic pressing (HIP). The evolution of mechanical properties and the micromechanisms of failure involved

were analysed as function of temperature (from 77 to 1473 K) and atmosphere (air and vacuum). The following conclusions were drawn from this study:

- The addition of both alloying elements produced a synergistic effect on microhardness reaching values significantly higher (around 12 GPa) than for pure W or previous alloys with only one of the elements added. Values were also 35 % higher than those obtained by other authors for materials produced by SPS. The effect on the elastic modulus, however, was unnoticeable since values remained almost invariable.
- Results from TPB tests showed that the addition of 4% V instead of 2% V did not contribute substantially to the improvement of the mechanical properties. Flexural strength results for both alloys were much higher than for pure W, they exhibited similar behaviour but a maximum of 1 GPa was obtained for W2V0.5Y alloy at 1273 K (a 30 % higher than for W4V0.5Y). Fracture toughness results were twice the values of pure W, but no significant differences were obtained between alloys.
- DBTT value for both alloys experienced a slight improvement, since ductile behaviour was not observed (before global degradation due to oxidation) in the case of pure W and was above 1073 K for the studied alloys; under vacuum, however, DBTT remained at the same temperature.
- In general, fracture surfaces were brittle in accordance with results from TPB tests without evidences of ductile behaviour. Fracture surfaces of test performed under vacuum exhibited mainly intergranular fracture by grain boundary decohesion, although some coarse grains in the fracture surfaces of the alloys exhibited transgranular fracture with cleavage even at higher temperatures.

Acknowledgements

This work has been carried out within the framework of the EUROfusion Consortium and has received funding from the Euratom research and training program 2014-2018 under grant agreement No 633053. The views and opinions expressed herein do not necessarily reflect those of the European Commission. The authors would also like to acknowledge to Ministerio de Economía y Competitividad of Spain project MAT2012-38541-C02-02 and Comunidad de Madrid (research project S2013/MIT-2862-MULTIMATCHALLENGE) for funding for this research. Special recognition is due to the "Departamento de Física de la Universidad Carlos III de Madrid" for providing the material use in this research.

References

[1] H. Bolt, V. Barabash, G. Federici, J. Linke, A. Loarte, J. Roth *et al*. J. Nucl. Mater. 307-311 (2002) 43-52.
[2] H. Bolt, V. Barabash, W. Krauss, J. Linke, R. Neu, S. Suzuki *et al*. J. Nucl. Mater. 329-333 (2004) 66-73.
[3] J. Hohe, P. Gumbsch J. Nucl. Mater. 400 (2010) 218-231.
[4] T. Palacios, A. Jimenez, A. Muñoz, M.A. Monge, C. Ballesteros, J.Y. Pastor J. Nucl. Mater. 454 (2014) 455-461.
[5] M.A. Monge, M.A. Auger, T. Leguey, Y. Ortega, L. Bolzono, E. Gordo *et al*. J. Nucl. Mater. 386-388 (2009) 613-617.
[6] W.C. Oliver and G.M. Pharr J. Mater. Res. 7 (1992) 1564-1583.
[7] ASTM C1259-98. Annual Book of ASTM Standards, American Society for Testing and Materials, West Conshohocken, Pennsylvania, 15.01 (1999) 386-400.
[8] Alger, Mark. S. M. (1997). Polymer Science Dictionary, Ed. Springer. ISBN 0412608707.
[9] ASM Handbook Vol 2 Properties and Selection: Nonferrous Alloys and Special-Purpose Materials. ASM International.
[10] O. Yeheskel and O. Tevet J. Am. Ceram. Soc. 82 (1999) 136–144.
[11] S. Timoshenko, Strength of Materials. D. Van Nostrand Company, 3rd Ed. 1955.
[12] T. Palacios, J.Y. Pastor. Influence of the notch root radius on the fracture toughness of brittle metals: nanostructure tungsten alloy, a case study. Submitted to Int. J. Refract. Met. Hard Mater.
[13] G. V. Guinea, J.Y. Pastor, J. Planas, M. Elices Int. J. Fract. 89 (1998) 103-116.
[14] T. Palacios, J.Y. Pastor, M.V. Aguirre, A. Martin, M.A. Monge, A. Muñoz *et al*. J. Nucl. Mater. 442 (2013) S277-S281.
[15] M.V. Aguirre Comportamiento mecánico de nuevas aleaciones de wolframio en función de la temperatura, PhD tesis, Universidad Politécnica de Madrid, 2014.
[16] K. Arshad, M-Y Zhao, Y. Yuan, Y. Zhang, Z-H Zhao, B. Wang *et al*. J. Nucl. Mater. 445 (2014) 96-100.
[17] T. Palacios, M.A. Monge, J.Y. Pastor. Tungsten-vanadium-yttria alloys for fusion power reactors (I): microstructural characterization, Submitted to J. Nucl. Mater.
[18] W. Webb, J. Norton, C. Wagner J. Electrochem. Soc. 103 (1956) 107-111.
[19] E. Kellett, S. Rogers J. Electrochem. Soc. 11 (1963) 502-504.